



The Photoluminescence and Ferromagnetic Behavior of Sprayed LaMnO_{2.75} thin Layers

A.Arrar^a, M. Benhaliliba^{b,c}, A. Boukhachem^d, A. Ayeshamariam^e

^aPhysical materials department, Ahmed ZABANA university centre, BP 48000, Relizane, Algeria.

^bPhysics Faculty, USTOMB University POBOX 1505 Mnaouer Oran Algeria.

^cFilm Device Fabrication-Characterization and Application FDFCA Research Group USTOMB, 31130 Oran Algeria.

^dUnité de physique des dispositifs a semi-conducteurs, Faculté des sciences de Tunis, Tunis El Manar University, 2092 Tunis, Tunisia.

^eDepartment of Physics, Khadir Mohideen College, Adirampattinam, Tamilnadu, India.

*Corresponding author. Arrar.physique@gmail.com. Tel. +213666102663

Received. January 01, 2019. Accepted. January 10, 2020. Published. March 19, 2020.

DOI: <https://doi.org/10.58681/ajrt.20040105>

Abstract. The study of Sr-doped lanthanum manganites (La_{1-x}Sr_xMnO_{2.75}, LSMO) with x= 0 and 0.4 are synthesized by spray pyrolysis method onto glass substrate at 460°C. The structural properties of the prepared samples are characterized by X-ray diffraction (XRD) technique and some parameters such as lattice parameters, crystallite size, microstrain and dislocation density have been reported. It is shown that LaMnO_{2.75}: Sr thin films crystallize in orthorhombic structure with a preferred orientation of the crystallites along (040) direction. In addition, atomic force microscopy (AFM) investigation displays the nanosphere aspect. UV-VIS-IR measurements show that the average transmittance of the LaMnO_{2.75}: Sr thin films is greater than 70% and optical band gap (E_g) of 2.85 eV is recorded. The photoluminescence (PL) measurements exhibit emission in the visible region, which is located at 530 nm. Finally, magnetic measurements at room temperature using vibrating sample magnetometer (VSM) technique reveal ferromagnetic behavior.

Keywords. La_{1-x}Sr_xMnO_{2.75}; LSMO; Sr doping; Structural properties; AFM; magnetic properties.

INTRODUCTION

Perovskite-based manganite have been the subject of intense research because of their complex magnetic and electric transport properties, especially in colossal magnetoresistance (CMR) (Hong et al., 2003).

The general formula for these types of manganite is $A_{1-x}B_xMnO_3$, where A is a rare earth atom and B is a divalent ion such as Sr, Ca or Ba (Nagaev, 2000).

LSMO possesses excellent physical properties, including high spin polarization, half-metallic-like conductivity, and good thermal stability, and spin charge and orbital ordering, which are suitable for applications in nanospintronic and nanoelectronic devices (Beltran-Huarac et al., 2013).

Indeed, this perovskite shows very promising magnetic activity and electromagnetic applications due to oxygen vacancies and cation excess, which are created for $LaMnO_x$ compounds (Dezanneau, 2003). These properties can be related to different oxidation numbers of manganese (Mn^{3+} and Mn^{2+}) which exist in the crystalline structure (Vincent et al., 2002).

Many different chemical methods have been developed for the synthesis of LSMO films including pulsed laser deposition (PLD) (Ishii et al., 2014), RF sputtering (Zongfan et al., 2016), sol gel (Danyan, 2015), hydrothermal method (Darko et al., 2013), solid-state reaction (Sakthipandi et al., 2013) and polymerizable complex method (Leandro et al., 2011).

The purpose of this study is to achieve the synthesis of $La_{1-x}Sr_xMnO_{2.75}$ ($x=0$ and 0.4%) thin films which are prepared onto glass substrate using the spray pyrolysis route at $460^\circ C$. Meanwhile, these films have been investigated by using XRD, atomic force microscopy, optical, photoluminescence and magnetic properties. Up to our knowledge no paper on Sr doped $LaMnO$ perovskite thin layers prepared by spray pyrolysis has been previously reported.

EXPERIMENTAL PROCEDURE

$La_{1-x}Sr_xMnO_{2.75}$ thin films with $x=0$ and 0.4 are prepared using spray pyrolysis method on glass substrates at $460^\circ C$ using 10^{-2} M of both aqueous solution of lanthanum chloride heptahydrate ($LaCl_3 \cdot 7H_2O$) and manganese chloride hexahydrate ($MnCl_2 \cdot 6H_2O$).

A high-resolution X-ray diffraction for X-ray patterns in the 2θ configuration is used with a copper anticathode ($CuK\alpha$, 1.54 \AA) using Philips PW 1729 system.

The transmittance spectra of the films are obtained using PerKin Elmer Lambda 950 spectrophotometer in 250-2500 nm wavelength range.

The PL spectra are performed at room temperature in 500-600 nm wavelength range.

Finally, the morphology of our sample is obtained with the atomic force microscope analyzer using the tapping mode.

RESULTS AND DISCUSSIONS

Structural characterization

The X-ray diffraction analysis of prepared of $LaMnO_{2.75}$: Sr perovskite samples is depicted in figure 1. X-ray diffraction spectra show well-defined peaks of (040), (141), (202) and (002), corresponding to orthorhombic phase according to JCPDS N° 00-035-1354 card.

Based upon X-ray analysis, it is obvious that the diffraction intensity has a tendency to decrease with an increase in the strontium doping level, and as-grown LSMO thin layers have preferential orientation along (040) direction.

In the LSMO structure, the d_{hkl} plane spacing is related to the lattice parameters a, b and c are calculated by using the following relation (Boukhachem et al., 2016):

$$\frac{1}{d_{hkl}^2} = \frac{h^2}{a^2} + \frac{l^2}{b^2} + \frac{l^2}{c^2} \quad (1)$$

Where h, k, l are the Miller indices. Moreover, the texture coefficient (TC) which indicates the maximum preferred orientation of the films along the diffraction plane means $T_C(hkl)$ values have been calculated from X-ray data, using formula (El-Nahass et al., 2004):

$$TC(hkl) = \frac{I_{(hkl)}/I_{0(hkl)}}{N^{-1} \sum I_{(hkl)}/I_{0(hkl)}} \quad (2)$$

Where $I_{(hkl)}$ is the measured relative intensity of (hkl) plane, $I_{0(hkl)}$ is the standard intensity, and N is the reflection number. The calculated values of $T_{C(hkl)}$ of the $\text{LaMnO}_{2.75}:\text{Sr}$ sprayed thin films are gathered in table 1.

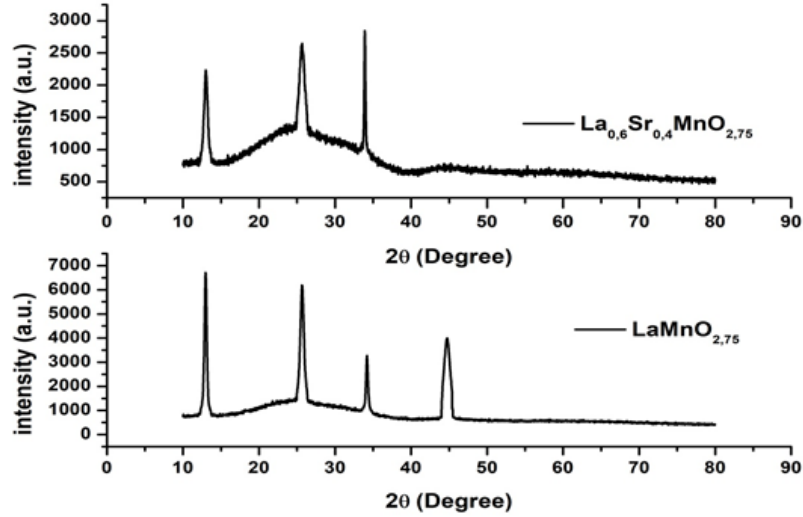


Fig. 1. X-ray diagram of pure and Sr-doped LMnO thin films prepared at 460°C.

Table 1. Lattice parameters and texture coefficient values of pure and Sr-doped $\text{LaMnO}_{2.75}$ thin layers.

	A (Å)	B (Å)	C (Å)	TC (040)
LaMnO_{2.75}	6.301	27.296	5.237	1.886
La_{0.6}Sr_{0.4}MnO_{2.75}	6.275	27.296	5.268	0.589

The crystallite sizes of LSMO are determined from full-width at half-maximum ($\beta_{1/2}$) and angle of diffraction (2θ) of the XRD peaks using Scherrer equation (Benouis et al., 2010):

$$D = \frac{k\lambda}{\beta_{1/2} \cos \theta} \quad (3)$$

Where λ ($=1.54 \text{ \AA}$) is the X-ray wavelength, $k=0.90$ is the Scherer constant. The grain size D values are estimated from (040) diffraction lines of $\text{LaMnO}_{2.75}:\text{Sr}$ sprayed thin films deposited at 460°C as indicated in table 2. It can be noted that the average crystallite grain size is found to be 47 nm for pure films. The crystalline size has a tendency to decrease with Sr doping.

Table 2. Grain size, dislocation density and microstrain of sprayed $\text{La MnO}_{2.75}:\text{Sr}$ thin layers.

	D (040) (nm)	δ (040) (10^{14} lines/m ²)	ϵ (040) (10^{-3})
LaMnO_{2.75}	47.77	4.382	6.43
La_{0.6}Sr_{0.4}MnO_{2.75}	34.12	8.587	9.01

The microstrain (ϵ), which is an interesting structural parameter of $\text{LaMnO}_{2.75}:\text{Sr}$ sprayed thin films is obtained using the following relation (Junaid et al., 2009):

$$\epsilon = \frac{\beta}{4 \tan \theta} \quad (4)$$

Where $\beta_{1/2}$ is the full-width at half-maximum of (040) peak and 2θ is the Bragg angle.

Finally, the dislocation density, defined as the length of dislocation lines per unit volume, has been estimated via the following equation (Jang et al., 2008):

37 $\delta = \frac{1}{D^2}$ (5)

The calculated dislocation density and micro strain of the samples are listed in tables 2. Finally, from this rapid calculation of structural constants, it can be seen that thin film based on LSMO perovskites exhibits some defaults such as dislocation and microstrain. This aspect is probably related to the low preparation temperature.

Surface morphology investigation

The surface morphology of deposited $\text{LaMnO}_{2.75}$: Sr films is examined by AFM ($5\mu\text{m} \times 5\mu\text{m}$) as shown in figure 2. The tridimensional atomic force microscopy (3D) image reveals that the surface of $\text{LaMnO}_{2.75}$ is composed with a nanosphere particle size. The grain size decreases with Sr-doping and surface becomes more homogenous. Such results corroborate with those reported in reference (Liu et al., 2016). A decrease is corresponding to a decrease in crystallization, which is firstly confirmed by XRD analysis as shown in figure 1.

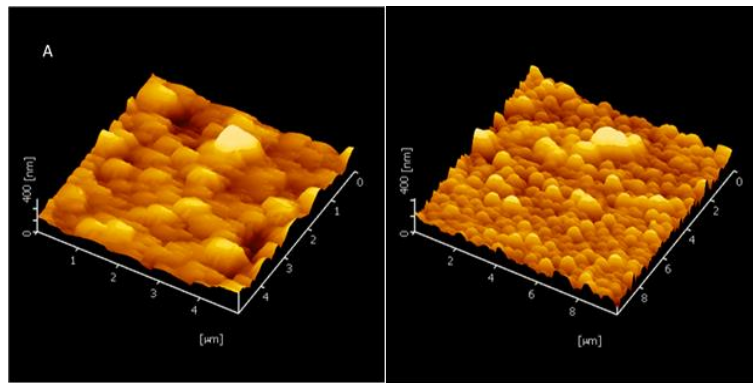


Fig. 2. 3D scanned AFM micrographs of (A) $\text{LaMnO}_{2.75}$ and (B) $\text{La}_{0.6}\text{Sr}_{0.4}\text{MnO}_{2.75}$.

Optical characterization

The transmittance spectra of $\text{LaMnO}_{2.75}$ pure and Sr-doped is depicted in figure 3.a. The transmittance shows a good transparency in the near infrared range ($>70\%$) which is important for transparent electronic applications.

The optical band gap can be extracted from the fundamental absorption edge of the films, which corresponds to electron transitions from valence band to conduction band. In the direct transition materials, the absorption coefficient (α) is expressed as follows (Keskenler et al., 2012):

$$\alpha h\nu = A(h\nu - E_g)^{1/2} \quad (6)$$

Where A is a dimensional constant, E_g the optical band gap. The extrapolation intercepting the photon energy axis gives the optical band gap E_g as shown in figure 3.b. It is found to be 2.85 eV and 2.84 eV for pure and 0.4 % Sr-doped films respectively as listed in table 3.

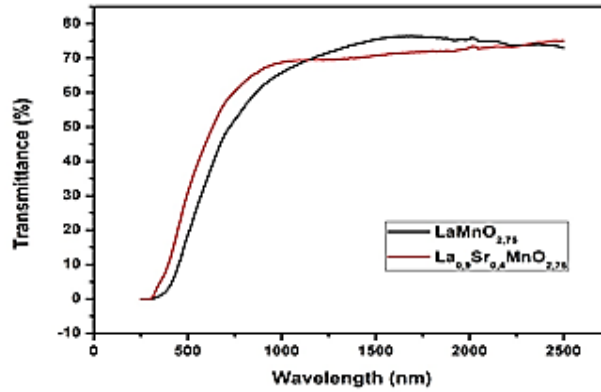


Fig. 3.a. Profile of transmittance spectra of La MnO_{2.75} : Sr thin films.

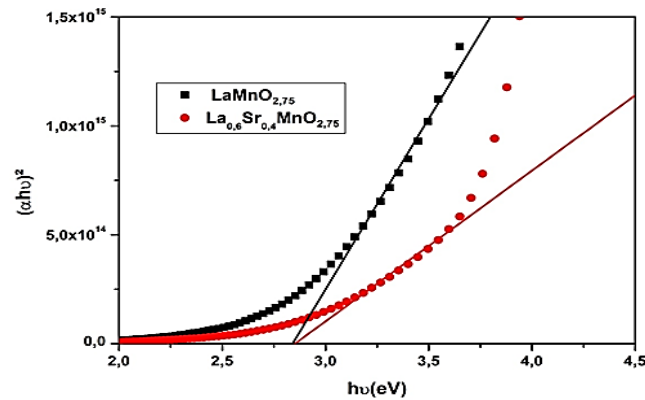


Fig. 3.b. Sketch of $(\alpha h\nu)^2$ vs. $h\nu$ for sprayed pure and Sr-doped LMnO thin films.

Table 3. Calculated values of optical band gap E_g of sprayed LaMnO_{2.75}:Sr thin layers.

	E_g (eV)
LaMnO_{2.75}	2.84
La_{0.6}Sr_{0.4}MnO_{2.75}	2.85

Photoluminescence characterization

Photoluminescence spectra of LaMnO_{2.75}: Sr thin films are shown in figure 4. It is observed that the La MnO_{2.75}: Sr exhibit a green emission band centered at 543 nm in range 500-600nm. From such measurement, it can see that 0.4% doping level seems good for luminescence in VIS range. This green emission in LaMnO_{2.75}: Sr sprayed thin films can be related to the transitions from the conduction band to the defect levels of O_{La}, O_{Mn} and O_i. Such as (O_i, O_{Ln/Mn}) is interstitial oxygen states.

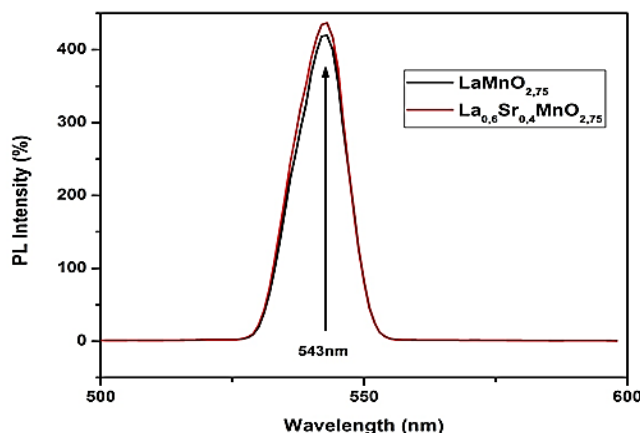


Fig. 4. PL spectra of sprayed $\text{LaMnO}_{2.75}:\text{Sr}$ thin films.

Magnetic characterization

In order to study the magnetic properties of the $\text{LaMnO}_{2.75}:\text{Sr}$ thin films the applied magnetic field (H) of 15 KOe, depending on the magnetization M (H), the magnetic hysteresis loop is measured and plotted as sketched in figure 5. The obtained result of $\text{LaMnO}_{2.75}:\text{Sr}$ sample is shown in figure 5. It is recorded that LSMO sample shows a sharp ferromagnetic to paramagnetic transition, which also further confirms the nature of single-phase of LSMO sample (Zi et al., 2009). It is clear after doping, that the sample shows a good ferromagnetic behavior at room temperature and the value of saturation magnetization (M_s) comes out to be 39 emu/g, which is similar to the previous results by the pyrophoric reaction process (Dutta et al., 2007).

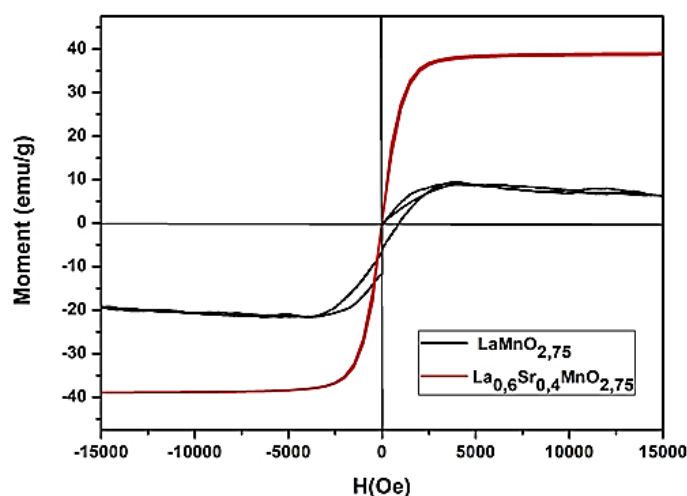


Fig. 5. Plot of magnetization vs. magnetic field of sprayed $\text{LaMnO}_{2.75}:\text{Sr}$ thin films.

CONCLUSION

In this work, $\text{LaMnO}_{2.75}:\text{Sr}$ thin films are prepared by the spray pyrolysis technique on glass substrates at 460°C . X-ray diffraction analysis shows that prepared films have orthorhombic phase and the crystallites are preferentially oriented along (040). The AFM observation reveals a nanospherical profile of particles. The optical study reveals a good transmittance in VIS-IR range with wide band gap equal to 2.85 eV. PL spectroscopy exhibits emission in VIS range. Finally, magnetic measurements show hysteresis loops leading to a ferromagnetic behavior of sprayed $\text{LaMnO}_{2.75}:\text{Sr}$ thin films.

REFERENCES

- Beltran-Huarac, J., Carpena-Nuñez, J., Barrionuevo, D., Mendoza, F., Katiyar, R. S., Fonseca, L. F., ... & Morell, G. (2013). Synthesis and transport properties of La_{0.67}Sr_{0.33}MnO₃ conformally-coated on carbon nanotubes. *Carbon*, *65*, 252-260.
- Benouis, C. E., Benhaliliba, M., Sanchez Juarez, A., Aida, M. S., Chami, F., & Yakuphanoglu, F. (2010). The effect of indium doping on structural, electrical conductivity, photoconductivity and density of states properties of ZnO films. *Journal of Alloys and Compounds*, *490*(1–2). <https://doi.org/10.1016/j.jallcom.2009.10.098>
- Boukhachem, A., Ziouche, A., Amor, M. ben, Kamoun, O., Zergoug, M., Maghraoui-Meherzi, H., Yumak, A., Boubaker, K., & Amlouk, M. (2016). Physical investigations on perovskite LaMnO_{3-δ} sprayed thin films for spintronic applications. *Materials Research Bulletin*, *74*. <https://doi.org/10.1016/j.materresbull.2015.10.003>
- Cao, D., Zhang, Y., Dong, W., Yang, J., Bai, W., Chen, Y., ... & Tang, X. (2015). Structure, magnetic and transport properties of La_{0.7}Ca_{0.3-x}Sr_xMnO₃ thin films by sol-gel method. *Ceramics International*, *41*, S381-S386.
- da Conceição, L., Ribeiro, N. F. P., & Souza, M. M. V. M. (2011). Synthesis of La_{1-x}Sr_xMnO₃ powders by polymerizable complex method: Evaluation of structural, morphological and electrical properties. *Ceramics International*, *37*(7). <https://doi.org/10.1016/j.ceramint.2011.03.069>
- Dezanneau, G., Sin, A., Roussel, H., Audier, M., & Vincent, H. (2003). Magnetic properties related to structure and complete composition analyses of nanocrystalline La_{1-x}Mn_{1-y}O₃ powders. *Journal of Solid State Chemistry*, *173*(1). [https://doi.org/10.1016/S0022-4596\(03\)00027-6](https://doi.org/10.1016/S0022-4596(03)00027-6)
- Duan, Z., Cui, Y., Shi, X., Wei, J., Ren, P., & Zhao, G. (2016). Facile fabrication of micro-patterned LSMO films with unchanged magnetic properties by photosensitive sol-gel method on LaAlO₃ substrates. *Ceramics International*, *42*(12). <https://doi.org/10.1016/j.ceramint.2016.06.021>
- Dutta, P., Dey, P., & Nath, T. K. (2007). Effect of nanometric grain size on room temperature magnetoimpedance, magnetoresistance, and magnetic properties of La_{0.7}Sr_{0.3}MnO₃ nanoparticles. *Journal of Applied Physics*, *102*(7).
- El-Nahass, M. M., Farag, A. A. M., Ibrahim, E. M., & Abd-El-Rahman, S. (2004). Structural, optical and electrical properties of thermally evaporated Ag₂S thin films. *Vacuum*, *72*(4). <https://doi.org/10.1016/j.vacuum.2003.10.005>
- Hong, X., Posadas, A., Lin, A., & Ahn, H. (2003). Ferroelectric-field-induced tuning of magnetism in the colossal magnetoresistive oxide La_{1-x}Sr_xMnO₃. *Physical Review B - Condensed Matter and Materials Physics*, *68*(13). <https://doi.org/10.1103/PhysRevB.68.134415>
- Ishii, K., Tachiki, M., Ooi, S., & Hirata, K. (2014). Fabrication of YBCO-LSMO-YBCO Lateral Structure with AFM Lithography. *Physics Procedia*, *58*. <https://doi.org/10.1016/j.phpro.2014.09.053>
- Jang, W. L., Lu, Y. M., Hwang, W. S., Hsiung, T. L., & Wang, H. P. (2008). Effect of substrate temperature on the electrically conductive stability of sputtered NiO films. *Surface and Coatings Technology*, *202*(22–23). <https://doi.org/10.1016/j.surfcoat.2008.06.025>
- Keskenler, E. F., Turgut, G., & Doğan, S. (2012). Investigation of structural and optical properties of ZnO films co-doped with fluorine and indium. *Superlattices and Microstructures*, *52*(1). <https://doi.org/10.1016/j.spmi.2012.04.002>
- Leandro, J., Simonsen, N., Saraste, J., Leandro, P., & Flatmark, T. (2011). Phenylketonuria as a protein misfolding disease: The mutation pG46S in phenylalanine hydroxylase promotes self-association and fibril formation. *Biochimica et Biophysica Acta - Molecular Basis of Disease*, *1812*(1). <https://doi.org/10.1016/j.bbadis.2010.09.015>

- Liu, G. Z., Yang, Y. Y., Qiu, J., Chen, X. X., Jiang, Y. C., Yao, J. L., ... & Gao, J. (2016). Substrate-related structural, electrical, magnetic and optical properties of La_{0.7}Sr_{0.3}MnO₃ films. *Journal of Physics D: Applied Physics*, 49(7), 075304.
- Makovec, D., Goršak, T., Zupan, K., & Lisjak, D. (2013). Hydrothermal synthesis of La_{1-x}Sr_xMnO₃ dendrites. *Journal of Crystal Growth*, 375. <https://doi.org/10.1016/j.jcrysgro.2013.04.019>
- Nagaev, E. L. (2000). A theory of colossal-magnetoresistance Pr-based manganites. *Physics Letters, Section A: General, Atomic and Solid State Physics*, 269(5–6). [https://doi.org/10.1016/S0375-9601\(00\)00272-3](https://doi.org/10.1016/S0375-9601(00)00272-3)
- Qazi, S. J. S., Rennie, A. R., Cockcroft, J. K., & Vickers, M. (2009). Use of wide-angle X-ray diffraction to measure shape and size of dispersed colloidal particles. *Journal of Colloid and Interface Science*, 338(1). <https://doi.org/10.1016/j.jcis.2009.06.006>
- Sakthipandi, K., Rajendran, V., & Jayakumar, T. (2013). Phase transitions of bulk and nanocrystalline La_{1-x}Sr_xMnO₃ (x = 0.35 and 0.37) perovskite manganite materials using in situ ultrasonic studies. *Materials Research Bulletin*, 48(4). <https://doi.org/10.1016/j.materresbull.2013.01.018>
- Vincent, H., Audier, M., Pignard, S., Dezanneau, G., & Senateur, J. P. (2002). Crystal Structure Transformations of a Magnetoresistive La_{0.8}MnO_{3-δ} Thin Film. *Journal of Solid State Chemistry*, 164(2), 177-187.
- Zi, Z. F., Sun, Y. P., Zhu, X. B., Yang, Z. R., Dai, J. M., & Song, W. H. (2009). Synthesis of magnetoresistive La_{0.7}Sr_{0.3}MnO₃ nanoparticles by an improved chemical coprecipitation method. *Journal of magnetism and magnetic materials*, 321(15), 2378-2381.